Int. J. Electrochem. Sci., 17 **(2022)** Article Number: 22012, doi: 10.20964/2022.01.23

International Journal of
ELECTROCHEMICAL
SCIENCE
www.electrochemsci.org

Corrosion Behavior of Bismuth in Concentrated Sulphuric Acid Solution and Stability of its Surface Oxide Film

A.S. Mogoda[1,*] *and K. M. Zohdy*[2]

[1] Chemistry Department, Faculty of Science, Cairo University, Giza 12613, Egypt
[2] Higher Technology Institute, Tenth of Ramadan City, Egypt
[*]E-mail: awad_mogoda@hotmail.com

Received: 3 August 2021 / *Accepted:* 4 October 2021 / *Published:* 6 December 2021

The surface activity of bismuth (Bi) was investigated in 4.97 M H_2SO_4 solution using cyclic voltammetry (CV), potentiodynamic polarization and electrochemical impedance spectroscopy (EIS) measurements. The CV results indicated that the current plateau values increase as the scan rate increases. This may be caused by the high ionic character of the protective film formed on Bi surface. From the EIS results it was found that the thickness of each of the pre-immersion oxide and the anodically formed film on Bi decreases with increasing of the immersion time due to their dissolution in the acid medium. Polarization scans showed that the rate of corrosion of Bi in the acid solution rises as the polarization temperature increases. The values of the thermodynamic parameters E_a (activation energy), ΔH (enthalpy change) and ΔS (entropy change) of the corrosion process for Bi in the concentrated sulphuric acid solution were estimated. The surface of bismuth was demonstrated under scanning electron microscopy (SEM) after polishing and polarization in sulphuric acid as well as at the end of the EIS measurements (at 70 min).

Keywords: Bismuth; cyclic voltammetry; EIS; polarization; SEM

1. INTRODUCTION

Bismuth has many applications in chemical pipes, alloy materials, flame retardants, electrocatalysis processes and military industries. Working improvement of lead (Pb)-acid battery was investigated using bismuth [1-5] since it is a component of Pb ores and is complicated to separate it from Pb. Bismuth oxide is characterized by a wide optical energy gap, a distinct light response and high refractive index [6-8]. Therefore, bismuth oxides have been used widely as fuel cells, sensor technology, ionic conductors and in the manufacture of superconducting materials [9-12]. In previous work, we investigated the stability of the anodic oxide film on bismuth in sulphuric acid which contains electroactive species [13], as well as the study of the electrochemical behavior of bismuth and its anodic

oxide film in phosphate solutions of various pH values [14]. Recently, the open circuit potential and the EIS studies for the mechanically polished bismuth in HCl solutions showed that the growth of the air-formed bismuth oxide proceeds on the surface in all the test solutions, but its thickness is reduced as the concentration of the acid increases [15]. The target of the present work is the investigation of the electrochemical behavior of bismuth and the stability of the anodic oxide film on its surface in 4.97 M sulphuric acid. The study was carried out using CV, polarization, EIS and SEM techniques.

2. EXPERIMENTAL

2.1. Sample and solution

Pure bismuth rod (99.99 %, BDH) was fixed into a glass tube with epoxy resin leaving surface area of 0.301 cm^2. Before immersion in the electrolyte, the bismuth electrode was polished using emery papers with various fine grades start from 600 down to 2000 grit, then rubbed with a soft cloth until it became a mirror-bright surface and washed with doubly distilled water. Sulphuric acid solution of concentration 4.97 M was prepared from highly pure chemical reagent (BDH) and doubly distilled water. The measurements have been carried out in naturally aerated solutions at 25 °C, except otherwise is stated.

2.2. Electrochemical tests

a glass double-jacket, three-electrode-cell was used in the present experiments. A platinum sheet was utilized as an auxiliary electrode. The potentials were measured versus Ag/AgCl electrode as a reference electrode. The measurements of CV, EIS, and polarization were carried out using the electrochemical workstation 1M6e zahner elektrik (Kronach, Germany). The impedance was measured at the input signal of 10 mV peak to peak in the frequency range 0.1-10^5 Hz [16,17].

2.3. Surface morphologies Characterization

The surface morphologies of bismuth and its anodic oxide film were examined by SEM (Quanta 250 FEG, Netherlands).

3. RESULTS AND DISCUSSION

3.1. Cyclic voltammetry measurements

Cyclic voltammograms of bismuth were recorded in the potential range from -1.6 to 1.8 V in 4.97 M H_2SO_4 solution using different scan rates as shown in Figure 1. The electrochemical processes occur through the anodic and cathodic parts of the bismuth voltammetric were reported previously [18] and here we are interested in the anodic part only.

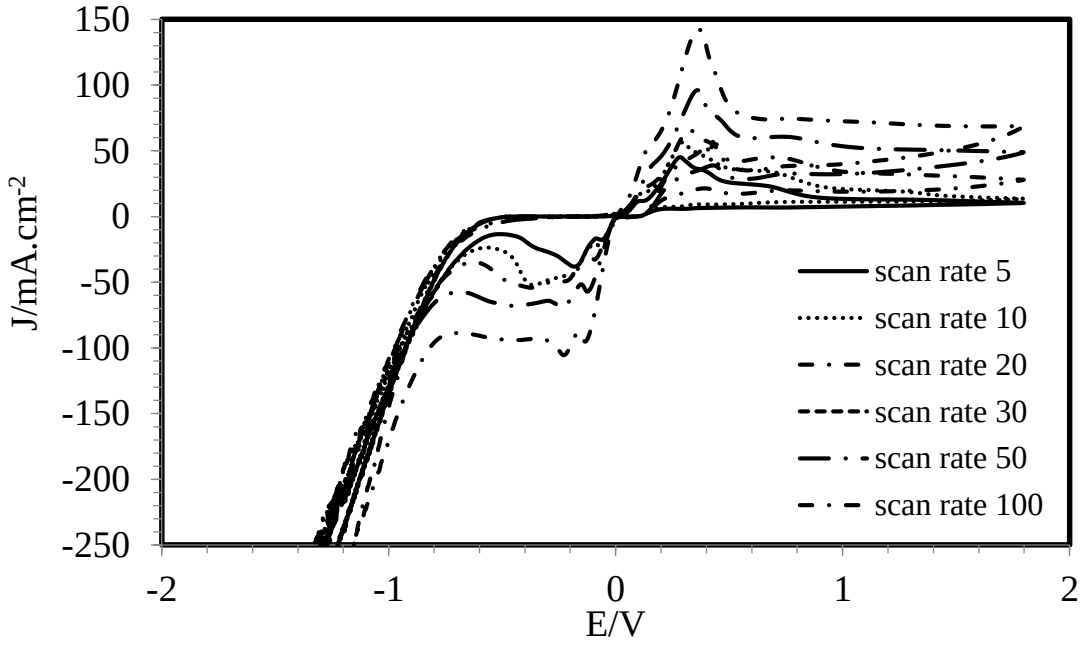

Figure 1. Cyclic voltammograms of Bi in 4.97 M H_2SO_4 at different scan rates in mV s^{-1}.

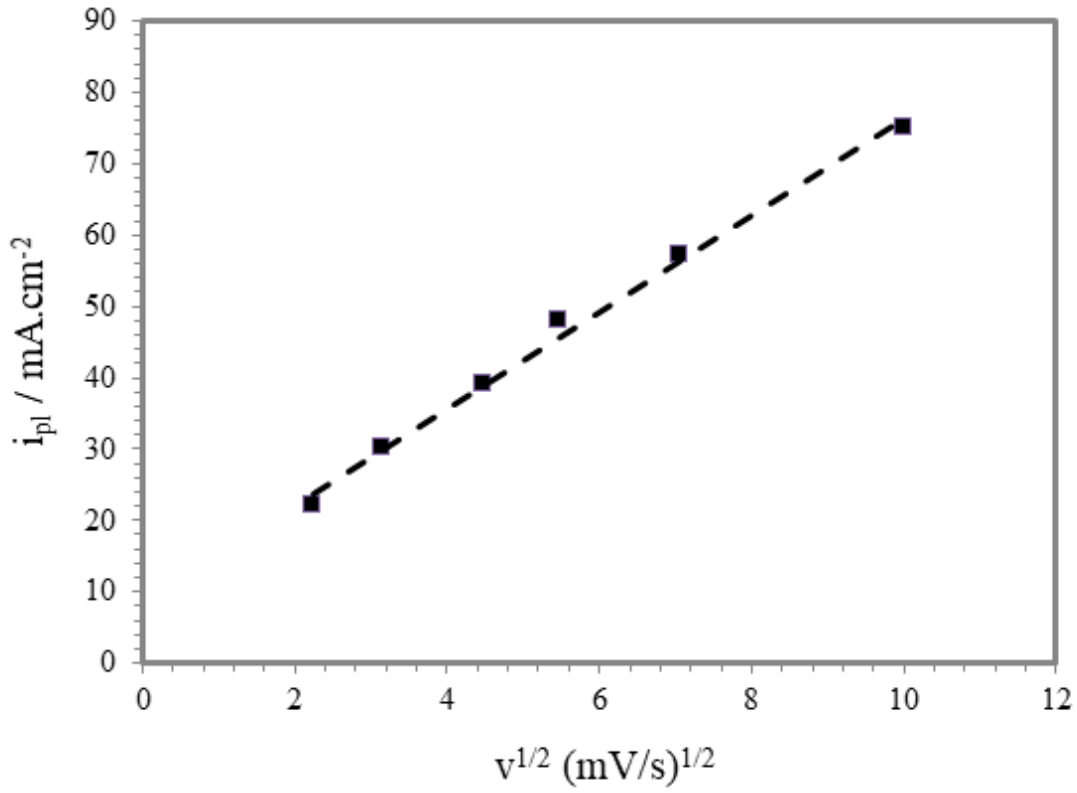

Figure 2. The plateau current as a function of the scan rate for Bi in 4.97 M H_2SO_4.

The anodic portion of bismuth voltammetric in Figure 1 reveals that the current increases with the increasing of the potential forming an anodic current peak and then stays almost constant. The height

of the current plateau gets long as the scan rate rises. The increase of current with potential can be explained by the active dissolution of Bi

$$Bi + H_2O = BiO^+ + 2H^+ + 3e^- \quad (1)$$

Increasing of BiO^+ ions concentration leads to formation of a monolayer of $(BiO)_2SO_4$ on Bi surface:

$$2BiO^+ + SO_4^{2-} = (BiO)_2SO_4 \quad (2)$$

The formation of this layer causes the decrease in the oxidation current with the appearance of the current peak as seen in Figure 1. As the potential increases, bismuth under the monolayer layer of $(BiO)_2SO_4$ undergoes oxidation:

$$Bi + 2H_2O = BiOOH + 3H^+ + 3e^- \quad (3)$$

The thickness of the BiOOH layer increases when the potential is increased.

The variation in the plateau current, $i_{pl,}$ with the square root of scan rate, $v^{1/2}$, for bismuth is a linear relationship as shown in Figure 2. This is in good consistent with the mechanism of a low-field migration for film growth [19,20]:

$$i = 2\ ABE \quad (4)$$

The ionic conductivity of the anodic layer on Bi surface is measured by the value of AB and the strength of the field E is given by:

$$E = (zF/V_m)\ (v/i_{pl}) \quad (5)$$

Where z is the metal ion valency, V_m is the molar mass of the anodic layer and F is the Faraday's constant. From equations (4) and (5) one can get:

$$i_{pl} = (2ABzF/V_m)^{1/2}\ v^{1/2} \quad (6)$$

The ionic conductivity of the anodic layer on bismuth was estimated from the slope of the straight line in Figure 2 and equation (6) and it was found to be 2.5×10^{-5} S cm^{-1}.

3.2. EIS measurements

3.2.1. For mechanically polished electrode surface

The impedance spectra of bismuth electrode were measured at different immersion times in 4.97 M H_2SO_4 solution. The experimental data are shown as Nyquist plots in Figure 3 and reveal that the diameter of the capacitive loop decreases with the increasing of the immersion time of bismuth in the acid solution. This means that the thickness of the air-formed film on the examined surface decreases with time because of its dissolution in H_2SO_4 solution. Figure 4 represents the equivalent electrical circuit used for fitting the EIS results obtained here. In the circuit, the components are as follows, R_s electrolyte resistance; C_{dl} capacitance of the double layer with constant phase element (CPE) behavior; R_{ct} resistance of the charge transfer for the metal corrosion; C_f surface film capacitance due to its dielectric nature; R_f resistance of the surface film.

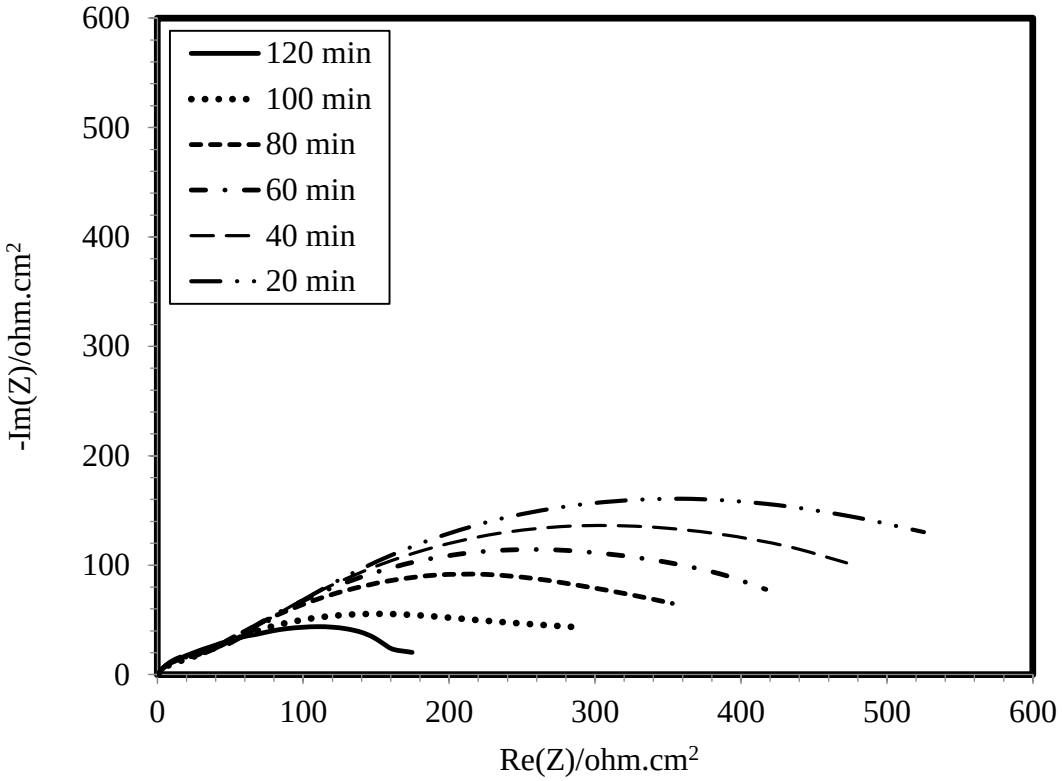

Figure 3. Nyquist plots of Bi in 4.97 M H_2SO_4 at different immersion times.

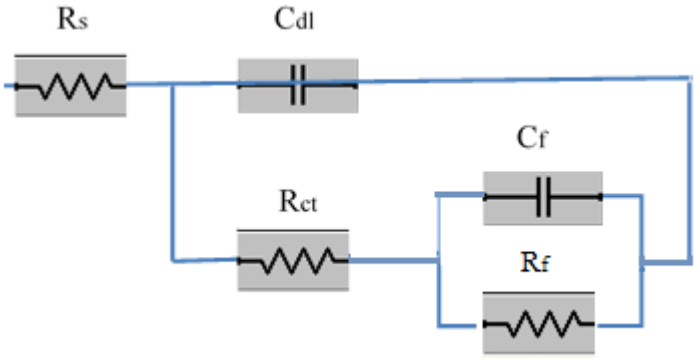

Figure 4. Equivalent circuit model for fitting the experimental EIS data.

Similar equivalent electrical circuit was obtained for TAV alloy in halide and azide anions [21], H_3PO_4 [22] and HBr [23]. Since the real capacitance differs from pure capacitance therefore, estimation of the impedance results can be performed by using a constant phase element (CPE) instead of the capacitance C. The impedance of CPE is expressed by the equation [24]:

$$Z_{CPE} = \frac{1}{N\,(j\,\omega)^n} \qquad (7)$$

where N is the real constant of the CPE which independent on the frequency and identical to the idealized capacitance at $\omega = 1$, ω is the angular frequency ($\omega = 2\pi f$ rad s^{-1}), $j = \sqrt{-1}$, and n is the coefficient related to deviation which varies between 1.0 for a purely capacitive behavior of a perfectly smooth

surface and 0.5 for a porous one [25]. The equivalent electrical circuit displays two-time constants owing to the surface film and the electrode/electrolyte interface. The fitted characteristic parameters for bismuth impedance in 4.97 M sulphuric acid are given in Table 1.

Table 1. The fitting parameters for the experimental impedance data of Bi in 4.97 M H_2SO_4 at different immersion times.

Time min	R_s ohm cm^2	R_f ohm cm^2	C_f µF cm^{-2}	n	R_{ct} ohm cm^2	C_{dl} µF cm^{-2}
20	2	505	1.26	0.83	55	22.9
40	2	440	1.46	0.82	53	26.7
60	2	375	3.00	0.85	52	32.9
80	2	310	4.45	0.84	50	41.4
100	2	270	4.74	0.86	48	44.9
120	2	145	4.75	0.85	45	47.8

From this Table it is obviously that the passive film resistance (R_f) decreases and consequently the capacitance of this film increases with the increasing of the immersion time of bismuth in the acid medium. The linear decreasing of R_f with time is clearly shown in Figure 5. This is a result of the thinning of the naturally formed protective film on Bi surface. Similar results were obtained for the mechanically polished Bi surface in H_2SO_4 of concentrations in the range from 0.0025 to 0.05 M where the reciprocal capacitance, which is an indication of oxide film thickness, decreases with time [26].

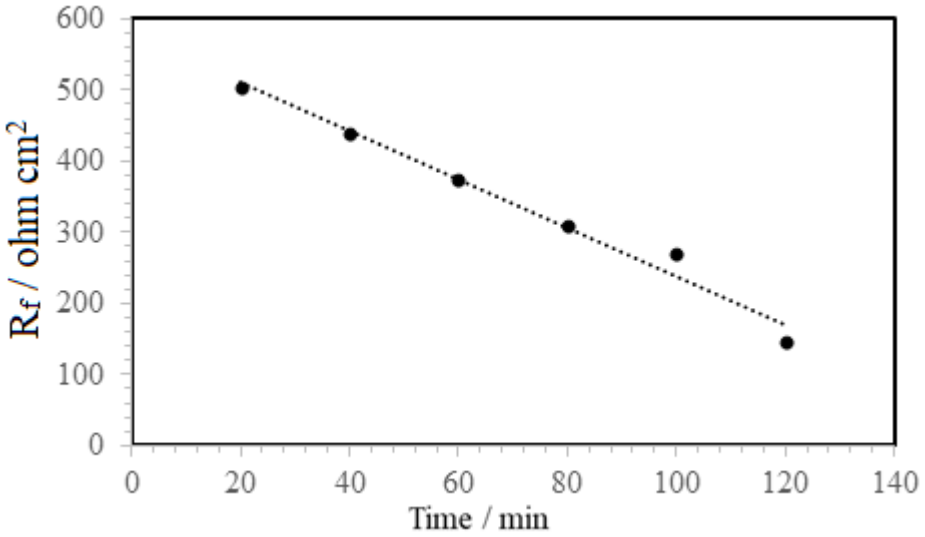

Figure 5. Variation of the resistance of the air formed passive film on Bi with immersion time in 4.97 M H_2SO_4.

3.2.2. For anodized bismuth surface

After anodic polarization of the mechanically polished surface of bismuth at a constant potential of 0.5 V for 20 min in 4.97 M H_2SO_4, the electrode was withdrawn from the polarization cell and

transferred to the freshly prepared 4.97 M H_2SO_4 solution where EIS was measured at different time intervals. The results in Figure 6 reveal that the semicircle diameter decreases with increasing the immersion time due to dissolution of the anodic passive film formed on Bi which is consistent with our previous results [13,14]. Also, Figure 7 shows that the value of film resistance, R_f, for the anodic formed film on bismuth decreases with time due to dissolution of this film on the metal.

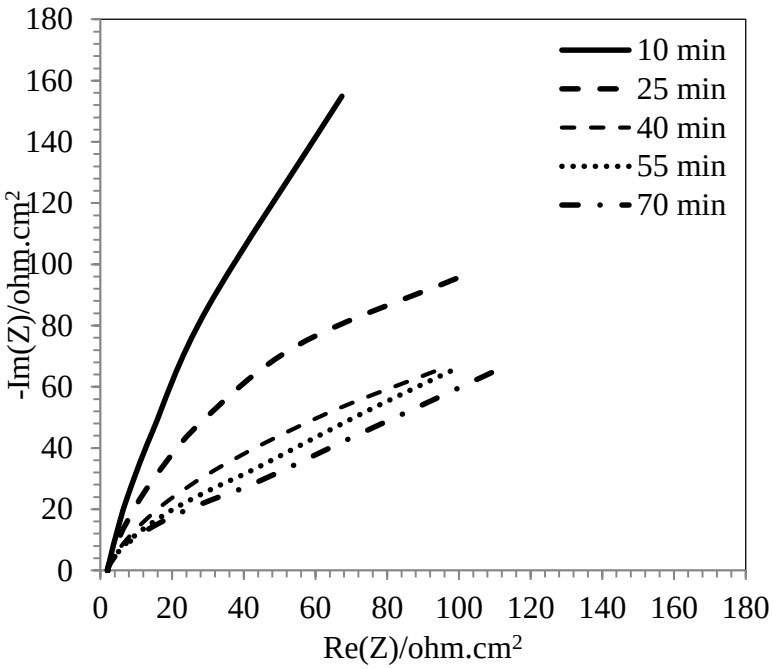

Figure 6. Nyquist plots of anodized bismuth surface in 4.97 M H_2SO_4 as a function of immersion time.

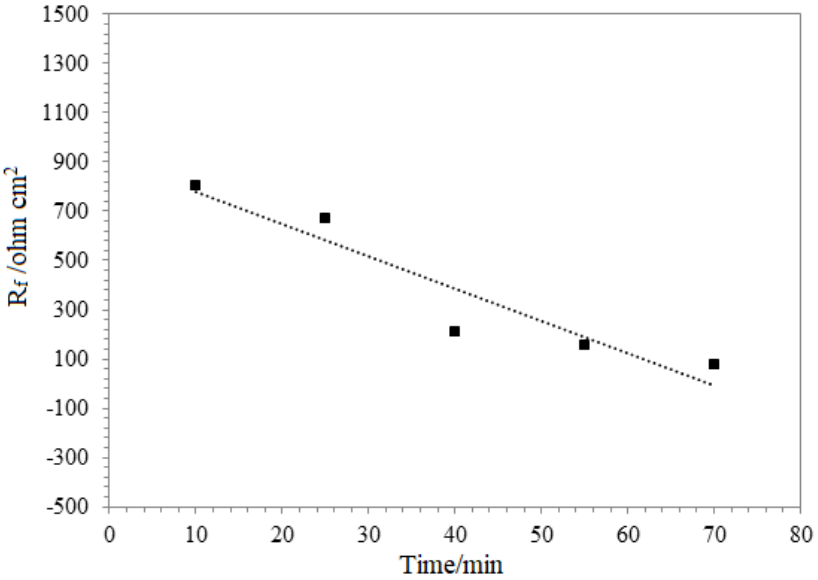

Figure 7. Variation of the film resistance, R_f, of the anodized bismuth surface with immersion time in 4.97 M H_2SO_4.

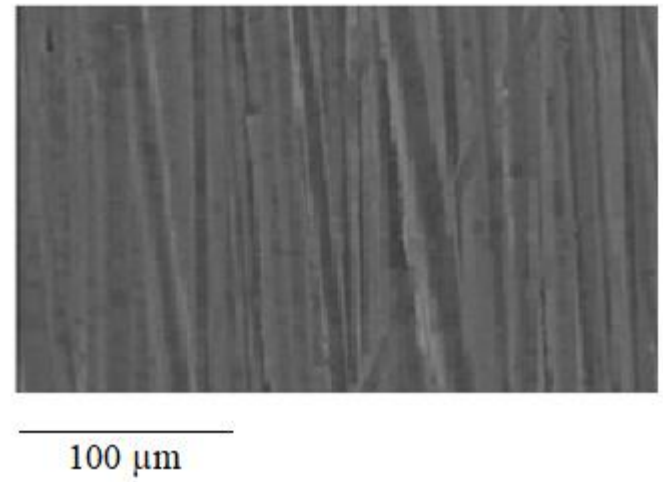

Figure 8. Micrographs of SEM for the (a) mechanically abraded Bi surface, (b) anodized Bi surface and (c) anodized Bi surface after immersion in 4.97 M H_2SO_4 for 70 min.

Recently, we used the SEM technique for investigation the surfaces of A 356 Al Alloy/ZrO_2 Composites in acid rain [27] and the surface of GO / CS /n-TCP composite which covered Co-Cr-W

alloy in serum [28]. The SEM micrograph for the mechanically abraded bismuth surface in Figure 8a displays the scratches and notches in the air-formed film on Bi which disappear by formation of the anodic oxide layer as seen in Figure 8b. On immersion the anodically formed film in the test solution the film exhibits from dissolution and the surface becomes not smooth as shown in Figure 8c.

3.3. Polarization measurements

Before starting the polarization experiments, bismuth was dipped in the acid solution till the open circuit potential was reached a steady state value. The potentiodynamic polarization curves of bismuth in 4.97 M H_2SO_4 solution at the various temperatures (25-65 ºC) are given in Figure 9.

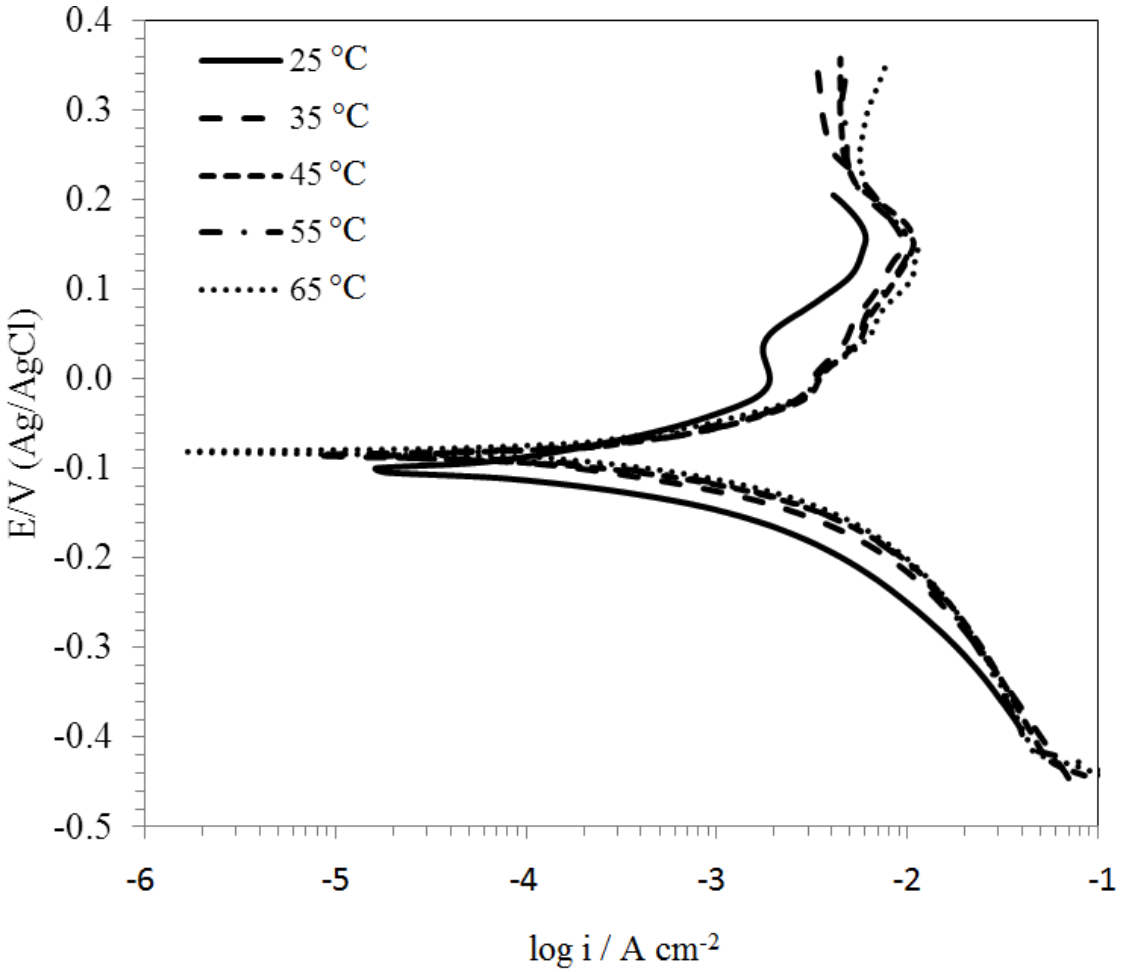

Figure 9. Potentiodynamic polarization curves of Bi in 4.97 M H_2SO_4 at different temperatures (scan rate, 10 mV s^{-1}).

The corrosion rate in mpy, $R_{corr,}$ corrosion current density, $I_{corr,}$ and corrosion potential, E_{corr}, of bismuth in the acid at the different temperatures are recorded in Table 2. These results proved that the corrosion rate of bismuth increases with increasing the polarization temperatures.

Table 2. The corrosion parameters of Bi in 4.97 M H_2SO_4 at different temperatures.

Temprature °C	E_{corr} mV	I_{corr} µA/cm^2	R_{corr} mpy
25	-98	4.64	2
35	-95	12.70	7
45	-98	15.80	8
55	-93	19.90	11
65	-100	43.40	23

Figure 10 shows that the relation between log I_{corr}, and temperature obeys the Arrhenius equation [29]:

$$\frac{d \log I_{corr}}{d\left(\frac{1}{T}\right)} = -\frac{E_a}{2.303\ R} \quad (8)$$

where E_a is the apparent activation energy of the corrosion process on Bi surface, R is the universal gas constant (8.314 J/mol K) and T is the absolute temperature (K).

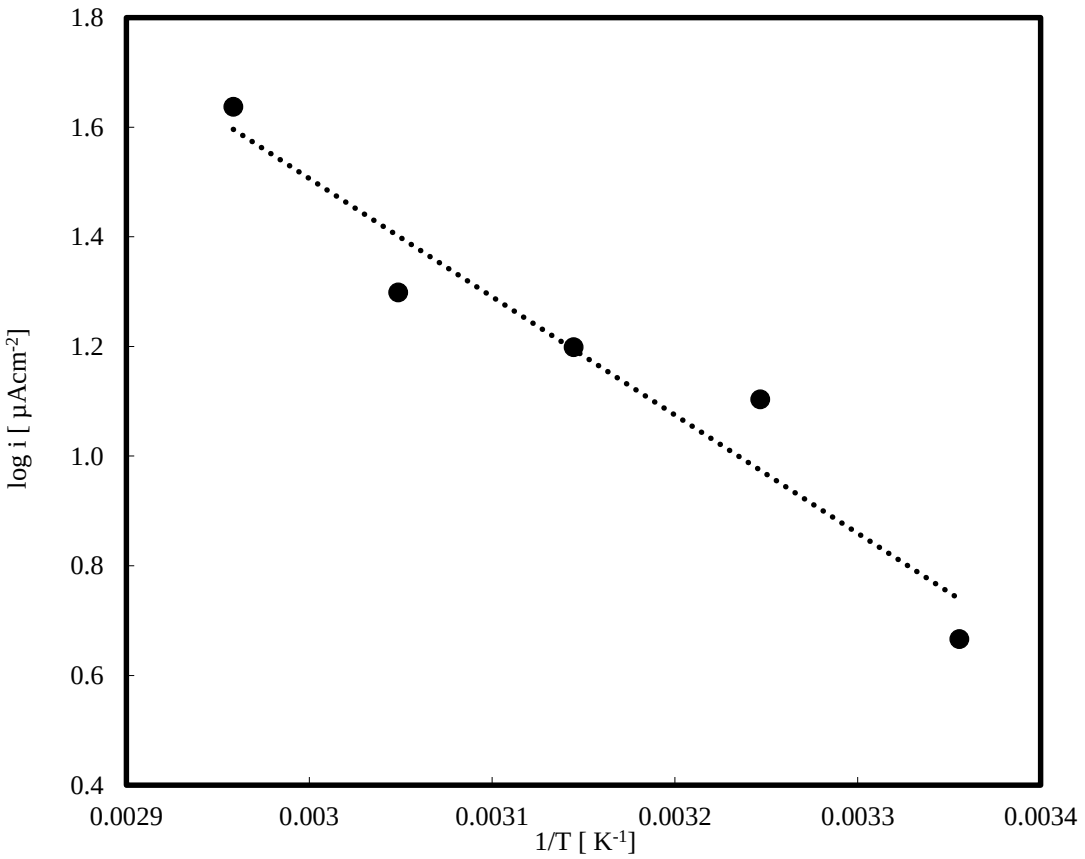

Figure 10. Arrhenius plot for the corrosion of Bi surface in 4.97 M H_2SO_4.

From the slope of the straight line in Figure 10 we calculated the value of E_a which equals 41.3 kJ/mol. The values of the change in enthalpy, ΔH, and the change in entropy, ΔS, for the corrosion process of bismuth in 4.97 M H_2SO_4 were found to be 38.7 kJ/mol and 96.6 kJ/mol K, respectively.

4. CONCLUSIONS

The results of CV for bismuth in 4.97 M H_2SO_4 displayed an active-passive peak with height increases with increasing of the scan rate and this peak followed with current plateau through which continuous growth of the anodic passive film occurs. The measurements of EIS at the open circuit potential revealed that the pre-immersion oxide film and the anodically formed film suffer from dissolution in the test solution. R_{corr} of bismuth in the acid solution was increased as the working temperature increased as manifested from the potentiodynamic polarization results. SEM micrographs revealed that the scratches and the defects that appeared in the mechanically polished bismuth surface were repaired by the anodic polarization of the metal in 4.97 M H_2SO_4 and the film formed was dissolved in the solution at the open circuit condition. The thermodynamic parameters E_a, ΔH, and ΔS were estimated.

References

1. J.E. Manders, L.T. Lam, R. De Marco, J.D. Douglas, R. Pillig and D.A.J. Rand, *J. Power Sources*, 48 (1994) 133.
2. L.T. Lam, N.P. Haigh, O.V. Lim, D. A.J. Rand and J.E. Manders, *J. Power Sources*, 78 (1999) 139.
3. L.T. Lam, N.P. Haigh, D.A.J. Rand and J.E. Manders, *J. Power Sources*, 88 (2000) 2.
4. L.T. Lam, N.P. Haigh and D. A.J. Rand, *J. Power Sources*, 88 (2000) 11.
5. W.S. Li, X.M. Long, J.H. Yan, J.M. Nan, H.Y. Chen and Y.M. Wu, *J. Power Sources*, 158 (2006) 1096.
6. T. Nikolov, M. Avoyo, E. Klein and K. Ikonopisov, *Thin Solid Films*, 30 (1975) 37.
7. V. Dolocan and F. Iova, *Phys. Stat. Sol*., A64 (1981) 755.
8. L. Leontie, M. Caraman, M. Alexe and C. Harnagea, *Surface Sciences*, 507 (2002) 480.
9. S. Arya and H. Singh, *Thin Solid Films*, 62 (1979) 353.
10. G. Bandoli, D. Barecca, E. Brescacin, G. Rizzi and E.Tondello, *Chem. Vap. Depos*., 219 (1996) 238.
11. V. Killedar and C. Bhosale, *Tr. J. Physics*, 22 (1998) 825.
12. T. Hyodo, E. Kanazawa, Y. Takao, Y. Shimizu and M.Egashira, *Electrochemistry*, 68 (2000) 24.
13. M. M. Hefny, A. S. Mogoda, S. A. Salih and H. E. El-Faiky, *Thin solid films* 204 (1991)193.
14. A. A. Ghoneim, A. S. Mogoda, M. A. Ameer and F. El-Taib Heakal, *Bull. Electrochem*., 12 (1996) 578.
15. A. S. Mogoda, *Bull.Mater.Sci*., 43 (2020) 100.
16. A.S. Mogoda and K.M. Zohdy, *Int. J. Electrochem. Sci.,* 15 (2020) 8070.
17. Reham H. Tammam, A. S. Mogoda and Mohamed H. Gharbawy, *Int. J. Electrochem. Sci.,* 15 (2020) 8408.
18. W.S. Li, X.M. Long, J.H. Yan, J.M. Nan, H.Y. Chen and Y.M. Wu, *J. Power Sources,* 158 (2006) 1096.
19. D. Williams and G.A. Wright, *Electrochim. Acta*, 21 (1976) 1009.

20. M. Bojinov, I. Kanazirski and A. Girginov, *Electrochim. Acta*, 40 (1995) 873.
21. F. El-Taib Heakal, A. A. Ghoneim, A. S. Mogoda and Kh. A. Awad, *Corros. Sci*., 53 (2011) 2728.
22. A.A. Ghoneim, A.S. Mogoda, K.A. Awad and F. El-Taib Heakal, *Int. J. Electrochem. Sci*., 7 (2012) 6539.
23. A. A. Ghoneim, F. El-Taib Heakal, A. S. Mogoda and K. A. Awad, *Surf. Interface Anal*., 42 (2010) 1695.
24. K. Juttner, *Electrochim. Acta*, 35(1990) 1501.
25. U.Rammelt and G. Reinhard, *Electrochim. Acta*, 35 (1990) 1045.
26. F. El-Taib Heakal, A.A. Mazhar and M.A. Ameer, *Br. Corros. J*., 23 (1988) 41.
27. A. S. Mogoda, K. M. Zohdy and M. A. Aboutabl, *Silicon*, doi.org/10.1007/s12633-021-01016-4.
28. Reham H. Tammam, A. S. Mogoda, H. H. Abo-almaged and Sara G. Abd El-Kader, *Int. J.Electrochem. Sci*., doi:10.20964/2021.12.13.
29. P. W. Atkins, "Physical Chemistry", 6th edn., *Oxford University Press* (1998) P. 864.